Gel-free experiments of reaction-diffusion front kinetics

Sung Hyun Park,[1] Stephen Parus,[1] Raoul Kopelman,[1] and Haim Taitelbaum[2]
[1]*Department of Chemistry, University of Michigan, Ann Arbor, Michigan 48109*
[2]*Department of Physics, Bar-Ilan University, Ramat-Gan 52900, Israel*

We present a gel-free experimental system to study the kinetics of the reaction front in the $A+B\rightarrow C$ reaction-diffusion system with initially-separated reactants. The experimental setup consists of a CCD camera monitoring the kinetics of the front formed in the reaction-diffusion process $Cu^{2+}+$ tetra [disodium ethyl bis(5-tetrazolylazo) acetate trihydrate] $\rightarrow$ 1:1 complex, in aqueous, gel-free solution, taking place inside a 150 μm gap between two flat microscope slides. The experimental results agree with the theoretical predictions for the time dependence of the front's width, height, and location, as well as the global reaction rate.

The kinetics of the reaction front in the $A+B\rightarrow C$ reaction-diffusion system with initially-separated reactants has been studied extensively in the past decade [1–31] and has shown many exotic properties. Initial separation of the reactants is an initial condition that readily enables, in principle, experimental investigations of this system [2,6,20,22,23]. Indeed, some of the novel characteristics of this system, such as the nonmonotonic motion of the reaction front [6], or the splitting of the front in the case of competing reactions [20], have been experimentally observed in a series of absorption measurements in a capillary where reactants diffuse and react in a gel solution.

However, some of the more recent theoretical predictions, such as the *complex* nonmonotonic motion of the reaction front [21] or the breakdown of the basic nonmonotonic motion [29] have not been obtained yet in experiments. This is attributable to experimental difficulties, some of them related to problems with the consistency of the gel solution.

In this Rapid Communication we present a gel-free experimental system and a set of measurements of the reaction front properties in this system. The reaction-diffusion processes are taking place in a confined geometry, within a gap of 150 μm between two flat microscope slides. Fibers of that diameter fill the boundary requirements for this experiment. These include a uniform gap easily assembled, ability to introduce reactants initially separated into this gap, and provide a means of controlled process initiation by removal of the boundary. A sketch of the experimental setup is shown in Fig. 1. A somewhat similar setup has been used very recently to study the dynamics of diffusion-limited corrosion of ramified electrodeposits [32].

The confined geometry of the experiment allows one to expect the system to be a non-convective one, with no need for a gel solution. In the current context, convection is any motion faster than diffusion, which may be characterized by a time exponent greater than 1/2. The old capillary experiments (52 cm long and 4 mm×2 mm cross section) were in fact three-dimensional, with the clear advantage of mean-field validity, but the necessity of the gel solution to prevent convection resulted in serious experimental difficulties [2,6,20,22,23].

The simple $A+B\rightarrow C$ system is assumed to be described for dimensions $d\geq 2$ by the mean-field equations for the local concentrations ρ_a, ρ_b, [1]

$$\frac{\partial\rho_a}{\partial t}=D_a\nabla^2\rho_a-k\rho_a\rho_b, \tag{1a}$$

$$\frac{\partial\rho_b}{\partial t}=D_b\nabla^2\rho_b-k\rho_a\rho_b, \tag{1b}$$

where D_a and D_b are the diffusion coefficients and k is the microscopic reaction rate constant. For the initially-separated system, the initial condition reads

$$\rho_a(x,0)=a_0H(x), \quad \rho_b(x,0)=b_0[1-H(x)], \tag{2}$$

where a_0, b_0 are the initial densities and $H(x)$ is the Heaviside step function, so that the A's are assumed to be initially uniformly distributed on the right side ($x>0$), and the B's on the left side ($x<0$) of the initial boundary.

The quantities that describe the kinetic behavior of the reaction front are defined on the basis of the reaction term $R(x,t)=k\rho_a(x,t)\rho_b(x,t)$. These are the front width $w(t)$ that was shown by Gálfi and Rácz [1] to increase with time as t^α, with $\alpha=1/6$, an exponent that is significantly smaller than the exponent 1/2 associated with the length scales in diffusion processes; the front height $R(x_f,t)$ that decreases with time as $t^{-\beta}$, $\beta=2/3$; and $x_f(t)$, the location of the reaction front center, which is defined as the position where $R(x,t)$ is maximal. This front location has been found [6,21]
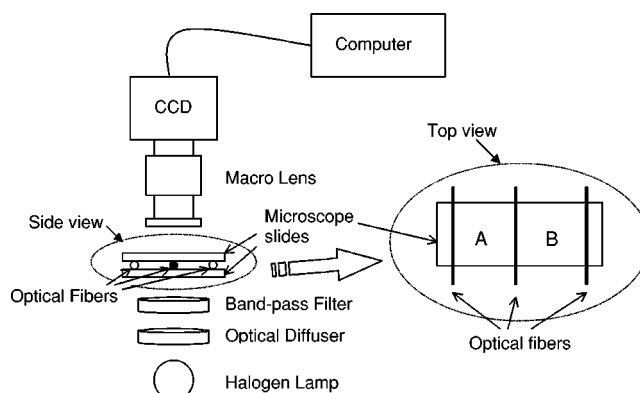

FIG. 1. A sketch of the experimental setup. The middle fiber is pulled out to initiate the reaction.
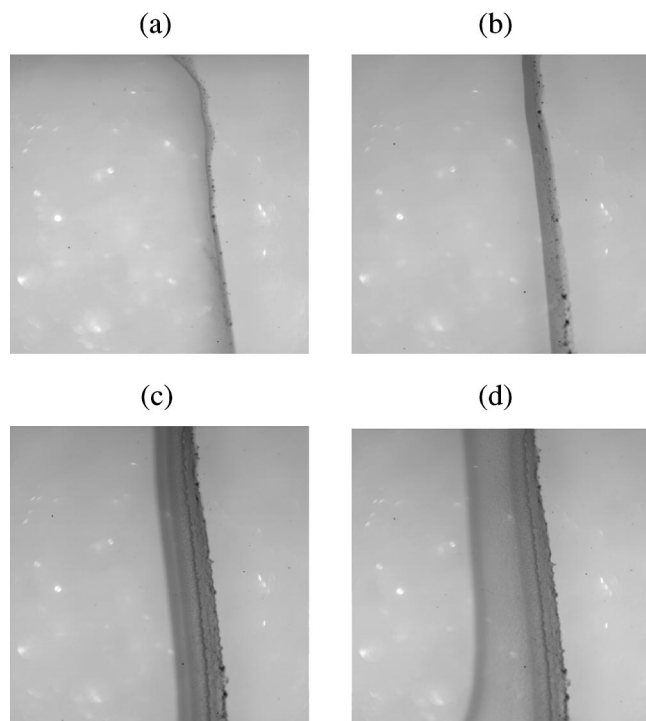
(a)   (b)

(c)   (d)

FIG. 2. Typical optical images of accumulated reaction fronts for the reaction-diffusion system Cu^{2+} (right)+tetra (left)$\rightarrow$1:1 complex. Images were taken at (a) 5 sec, (b) 2 min, (c) 25 min, and (d) 44 min, after the initiation of the process.

to behave in a nontrivial manner, prior to the asymptotic propagation as $t^{1/2}$. The global reaction rate, $R(t)$, is just the integrated area under $R(x,t)$, and it goes asymptotically as $t^{-1/2}$.

In the following we describe in detail the experimental setup and procedure and present data for the above-mentioned quantities, which have been found to be in good agreement with the theoretical predictions.

The experiments are performed in a thin gap (about 150 μm) between two flat microscope slides with dimensions 75 mm$\times$25 mm$\times$1 mm. Three parallel optical fibers with a diameter of 150 μm are inserted between the two microscope slides as shown in Fig. 1. Two optical fibers at both ends act as spacers, while the fiber at the center of the slides acts as a boundary, allowing the initial separation of the two reactant solutions, as well as the formation of a straight reaction front at $t=0$. The observed reaction is a 1:1 complex formation between copper (II) and disodium ethyl bis(5-tetrazolylazo)acetate trihydrate (''tetra'') in aqueous solution, i.e., Cu^{2+}+tetra$\rightarrow$1:1 complex. The concentrations of the reactants are $[Cu^{2+}]=2\times10^{-3}M$ and $[$tetra$]=1\times10^{-3}M$. The reactants are injected with syringes into each side of the thin gap.

A CCD camera (SpectraSource Instruments, model Teleris 2 12/16) with a macrolens (Nikon AF Micro 60 mm f2.8 1:1) records the optical absorption images of the product at different times. The CCD has 512$\times$512 pixels, and the size of the image monitored is $\approx$1 cm$\times$1 cm, so the spatial resolution is $\approx$20 μm/pixel. A typical exposure time is 100 ms.
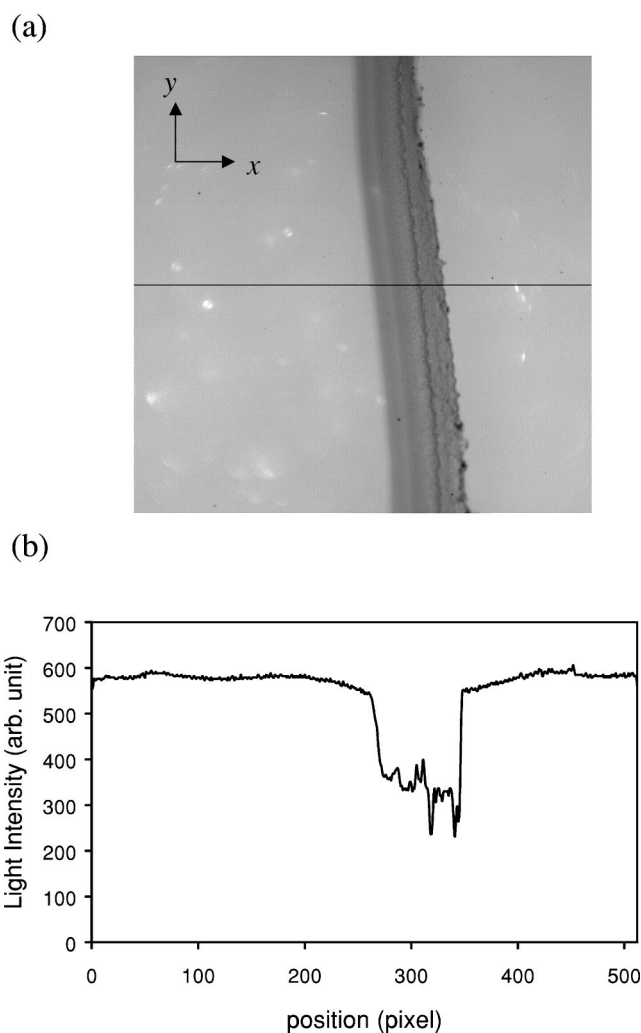
(a)

(b)

FIG. 3. (a) A typical absorption image of the reaction front in the experiment, with a coordinate system added, taken at $t=25$ min. The horizontal line represents a pixel line at $y=256$. (b) The corresponding transmission profile of the product along the pixel line.

An optical diffusing glass reduces spatial fluctuations of the light intensity from the halogen lamp over the illumination area. The absorption maximum of the purple-colored product is 535 nm, whereas the absorption of the tetra reactants is peaked at 410 nm. An optical band-pass filter at 540 nm monitors only the product, where the reactants have negligible absorption and are not observed in the images. The entire experiment is performed at room temperature.

After the reactants are injected into the gap between the slides, the fiber at the center of the slides is pulled out quickly to initiate the reaction. The reaction results in the immediate formation of the purple-colored product at the boundary. The first image of the product is taken immediately when the optical fiber is removed from the center of the slides (time zero). A series of images of the product are then taken with time intervals increasing from 30 sec to 20 min. Product formation was typically monitored up to about 60 min. It was not necessary to have a boundary or seal the long
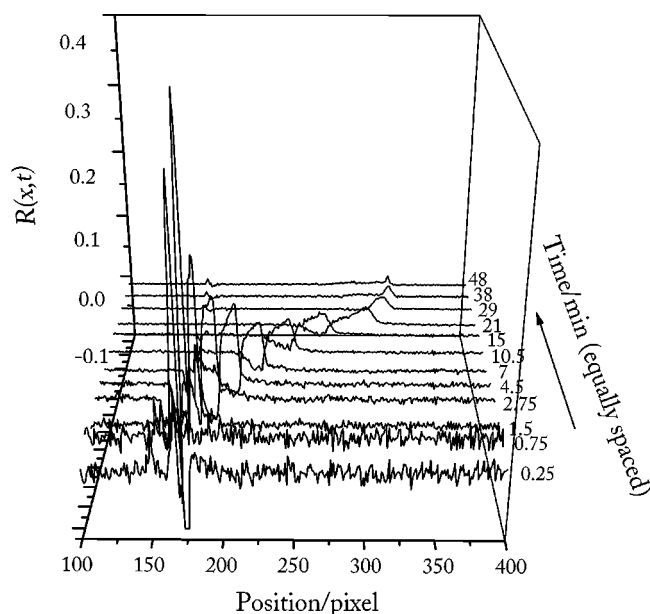
FIG. 4. A typical pattern of evolution of the reaction front profile at successive times, 0.25–48 min (not in scale).

FIG. 5. Reaction front kinetic characteristics as a function of time. (a) Center, (b) width, (c) height, (d) global reaction rate.

edge of the slide, since no evaporation effects were observed from these water-based solutions over the time of the reaction.

Figure 2 shows typical images of the product seen as the dark vertical band for a series of successive times (ranging from 5 sec up to 44 min). Copper ions are on the right side and tetra ions are on the left of the product in the image. This image represents the total accumulated product formed up to that time. To obtain the mean-field properties of the dynamics of the reaction front in our experimental system, one has to integrate the product intensities along the y axis that is parallel to the reactant boundary. However, noticing the similarity of the product concentrations along the y axis in the image, it can be assumed that, in principle, the dynamics along the y axis is independent of position, and no integration along the y axis is required. This symmetry allows one to choose any one pixel line along the x axis and compare the profiles at this position within the series of images. Figure 3(b) shows a typical product profile along the $y=256$ pixel line from the image in Fig. 3(a), obtained at $t=25$ min.

According to the Beer-Lambert law, the absorption in Fig. 3(b) is directly proportional to the concentration of the product. Subtracting two consecutive profiles of the product and normalizing by the time interval between them, we obtain the profiles of the reaction front at different times along the line we select ($y=256$ in this case), i.e., the spatial profiles of $R(x,t)$ at different times. In Fig. 4 we show a set of reaction profiles corresponding to the production rate $R(x,t)$ of C at successive times, ranging from 15 sec up to 48 min. We can then measure the dynamic parameters of the reaction front from the profiles, namely, the position of the reaction front, $x_f(t)$, the width $w(t)$, the height at the front center, $R(x_f,t)$, and the global reaction rate, $R(t)$.

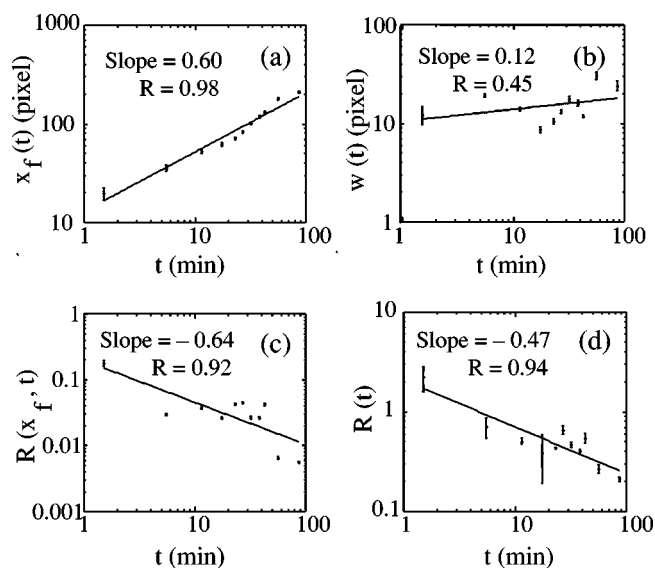Although analysis of the front properties of a single pixel line seems to be sufficient, one can achieve better statistics by repeating the aforementioned data processing procedures at more horizontal pixel lines. We have then taken the average of the measurements of the dynamic parameters from 15 pixel lines ($y=160$, 165, 170, 175, 180, 190, 195, 200, 205, 210, 226, 236, 246, 256, and 266), to obtain the averages of center location, width, and height of the reaction front at different times, as well as the global reaction rate. In Fig. 5 we plot the results of this analysis. The time exponents seem to be in good agreement with the theory. The exponent for the center location of the reaction front, $x_f(t)$, is found to be 0.60, which is slightly higher than the theoretical 1/2, but the results for the width and the height, 0.12 and -0.64, respectively, are reasonably close to the theoretical values $\alpha=1/6$ and $\beta=-2/3$. In addition, they obey the scaling relation for these exponents, which was shown by Gálfi and Rácz [1] to be $\alpha+\beta=-1/2$. An independent calculation of the global reaction rate yields the exponent -0.47, in agreement with the theoretical value $-1/2$.

In summary, we have presented an alternative experimental system for reaction-diffusion kinetics with initial separation geometry. The system reproduces the basic anomalous kinetics of this process. The technique, in particular the use of a gel-free solution in which the reaction takes place, is very promising. It can be utilized for other investigation techniques, such as fluorescence, with the advantage of better signal-to-noise ratio. In particular, one can try to control the motion of the reaction front by changing the initial concentrations, in order, for example, to stabilize the front motion, or to have it moving in any preferred direction after possible nonmonotonic motion. In addition, further reducing the gap size may eliminate any possible convection effects.

[1] L. Gálfi and Z. Rácz, Phys. Rev. A **38**, 3151 (1988).

[2] Y-E.L. Koo and R. Kopelman, J. Stat. Phys. **65**, 893 (1991).

[3] Z. Jiang and C. Ebner, Phys. Rev. A **42**, 7483 (1990).

[4] H. Taitelbaum, S. Havlin, J.E. Kiefer, B. Trus, and G.H. Weiss, J. Stat. Phys. **65**, 873 (1991).

[5] S. Cornell, M. Droz, and B. Chopard, Phys. Rev. A **44**, 4826 (1991).

[6] H. Taitelbaum, Y-E.L. Koo, S. Havlin, R. Kopelman, and G.H. Weiss, Phys. Rev. A **46**, 2151 (1992).

[7] M. Araujo, S. Havlin, H. Larralde, and H.E. Stanley, Phys. Rev. Lett. **68**, 1791 (1992).

[8] E. Ben-Naim and S. Redner, J. Phys. A **25**, L575 (1992).

[9] H. Larralde, M. Araujo, S. Havlin, and H.E. Stanley, Phys. Rev. A **46**, 855 (1992); **46**, R6121 (1992).

[10] S. Cornell and M. Droz, Phys. Rev. Lett. **70**, 3824 (1993).

[11] M. Araujo, H. Larralde, S. Havlin, and H.E. Stanley, Phys. Rev. Lett. **71**, 3592 (1992).

[12] B. Chopard, M. Droz, T. Karapiperis, and Z. Rácz, Phys. Rev. E **47**, R40 (1993).

[13] B.P. Lee and J. Cardy, Phys. Rev. E **50**, R3287 (1994); J. Stat. Phys. **80**, 971 (1995).

[14] M. Howard and J. Cardy, J. Phys. A **28**, 3599 (1995).

[15] S. Cornell, Phys. Rev. E **51**, 4055 (1995).

[16] S. Cornell, Z. Koza, and M. Droz, Phys. Rev. E **52**, 3500 (1995).

[17] M. Araujo, Physica A **219**, 239 (1995).

[18] G.T. Barkema, M.J. Howard, and J.L. Cardy, Phys. Rev. E **53**, R2017 (1996).

[19] Z. Koza, J. Stat. Phys. **85**, 179 (1996); Physica A **240**, 622 (1997).

[20] H. Taitelbaum, B. Vilensky, A. Lin, A. Yen, Y-E.L. Koo, and R. Kopelman, Phys. Rev. Lett. **77**, 1640 (1996).

[21] Z. Koza and H. Taitelbaum, Phys. Rev. E **54**, R1040 (1996).

[22] A. Yen, Y-E.L. Koo, and R. Kopelman, Phys. Rev. E **54**, 2447 (1996).

[23] H. Taitelbaum, A. Yen, R. Kopelman, S. Havlin, and G.H. Weiss, Phys. Rev. E **54**, 5942 (1996).

[24] V. Malyutin, S. Rabinovich, and S. Havlin, Phys. Rev. E **56**, 708 (1997).

[25] B. Chopard, M. Droz, J. Magnin, and Z. Rácz, Phys. Rev. E **56**, 5343 (1993).

[26] Z. Koza and H. Taitelbaum, Phys. Rev. E **56**, 6387 (1997).

[27] H. Taitelbaum and Z. Koza, Philos. Mag. B **77**, 1389 (1998).

[28] M. Sinder and J. Pelleg, Phys. Rev. E **60**, R6259 (1999); **61**, 4935 (2000); **62**, 3340 (2000).

[29] H. Taitelbaum and Z. Koza, Physica A **285**, 166 (2000).

[30] M.Z. Bazant and H.A. Stone, Physica D **147**, 95 (2000).

[31] J. Magnin, Eur. Phys. J. B **17**, 673 (2000).

[32] C. Leger, F. Argoul, and M.Z. Bazant, J. Phys. Chem. B **103**, 5841 (1999).